RESEARCH ARTICLE

Magneto hydrodynamic (MHD) pulsatile motion of blood with wall slip velocity and periodic body acceleration

Ruma Bagchi, Anup Kumar Karak*

ABSTRACT

Background: The present investigation is concerned with the theory of a model of the pulsatile motion of blood through a mild stenosed long tube under the influence of a uniform transverse magnetic field and periodic body acceleration. *Methods:* In the present investigation, a mathematical model has been developed to study the effect of externally applied uniform transverse magnetic field on blood motion through stenosed vessels, considering slip velocity at the vessel's endothelium. *Results:* To analyze the problem, blood is assumed to be incompressible and Newtonian homogeneous fluid as far as large arteries' shear rate is high. Noting the behavior of red cells in the arteries, the possibility of the role of slip velocity at the wall under certain conditions has been considered. Also, since for biological systems, blood is conducted with a low magnetic Reynolds number, the flow is supposed to be under the action of a uniform magnetic field for which the induced magnetic field can be neglected. Moreover, the pulsatile motion is generated by sinusoidal behavior and is affected by periodic body acceleration. Exact solutions of the relevant equations are obtained using Laplace and Hankel integral transforms. *Conclusion*: The expressions for axial velocity, flow rate, fluid acceleration, and shear stress are given in analytical for us. The effects of magnetic field and body acceleration on the solutions have been discussed graphically. The present study seems to immerse importance in diversified fields of biomedical engineering.

Keywords: Pulsatile flow of blood, Body acceleration, Magnetic field, Laplace, Finite Hankel transforms.

Indian Journal of Physiology and Allied Sciences (2025); DOI: 10.55184/ijpas.v77i02.311 **ISSN:** 0367-8350 (Print)

INTRODUCTION

Localized narrowing in a blood vessel is termed stenosis in medical science. Many cardiovascular diseases, particularly in mammalian arteries, are closely related to the nature of blood movement and the dynamic behavior of blood vessels and, in their severe form, lead to morbidity and fatality. However, the mechanism of development of stenosis in the lumen of the artery is not yet known, but various researchers emphasized that some of the major factors for the development of this vascular disease are due to the formation of intravascular plaques and the impingement of ligaments and spurs on the blood vessel wall.[1-5] Moreover, the blood flow characteristics are significantly altered in the vicinity of the stenotic region, and many abnormalities arise in the flow pattern. Some experiments on models of arterial stenosis have been carried out by Young,[2] and it was noted that the changed behavior of the blood flow might have a coupling effect on the further development of vascular disease. Various investigators[6-10] opined that the study of different hydrodynamic factors like skin friction and pressure under normal physiological conditions and in pathological states may provide useful information regarding pathogenesis and the proper treatment of various arterial diseases like myocardial infarction, stroke, etc.

Various mathematical models of blood flow through stenosed blood vessels have been developed by several researchers [2,11-13] of which Young's work[2] may be considered a pioneer. Sanyal *et al*. employed numerical techniques to study the blood flow through an astenosed tube.[12] Although blood is a non-Newtonian suspension of cells in plasma, Chaturani and Biswas observed that for vessels of a radius greater than 0.25 mm, it may be considered a homogeneous Newtonian fluid.[5] At lower shear rates, blood exhibits non-Newtonian behavior,[14] but for larger arteries, blood may be considered as Newtonian fluid[15] because the shear rate is high for these. It is worth mentioning that most of the aforementioned studies relating to stenosis models are based on the assumption of no-slip condition at the vessel wall. However, based on *in-vitro* experiments to study the behavior of red cells during blood flow, Benneth[16] pointed out that the red cells might have a slip velocity at the wall under certain conditions. Subsequently, several investigators[17-19] also indicated the possibility of slip velocity at the inner surface of the wall. On the other hand, Vardanyan[20] reported that biological systems, in general, are affected by the application of an external transverse magnetic field which is corroborated by Das and Saha.[21]

In the present investigation, a mathematical model has been developed to study the effect of externally applied

Department of Mathematics, Berhampore Girls' College, Berhampore, Murshidabad 742101, West Bengal, India.

***Corresponding author:** Anup Kumar Karak, Department of Mathematics, Berhampore Girls' College, Berhampore, Murshidabad 742101, West Bengal, India., Email: karakanup99@gmail.com

How to cite this article: Bagchi R, Karak AK. Magneto hydrodynamic (MHD) pulsatile motion of blood with wall slip velocity and periodic body acceleration. *Indian J Physiol Allied Sci* 2025;77(2):35-43.

Conflict of interest: None

Submitted: 05/08/2024 **Accepted:** 08/03/2025 **Published:** 20/06/2025

uniform transverse magnetic field on blood motion through stenosed vessels, considering slip velocity at the vessel's endothelium. Blood has been considered to be Newtonian, incompressible conducting fluid, and the flow is laminar. The stenosis is supposed to be mild. The analytical expressions are computed numerically to quantify the extent to which the slip velocity and the magnetic field can influence the blood flow pattern of blood vessels. Moreover, the motion is pulsatile, developed by the sinusoidal behavior of pressure gradient, and is affected by periodic body acceleration. Laplace and finite Hankel transforms have been used to solve the problem. It is noted that the effects of the magnetic field may have some consequences in these types of situations, for example, during MRI scanning.

Mathematical Formulation of the Problem

Let us consider the axially symmetric and fully developed pulsatile motion of blood through a stenosed artery with body acceleration. Blood is assumed to be Newtonian and incompressible conducting fluid. Also, the artery is a long cylindrical tube with an axis along the z-axis. The pressure gradient and body acceleration are assumed to be represented

$$-\frac{\partial P}{\partial z} = A_0 + A_1 \cos\left(\omega_p t\right) \tag{1}$$

$$G = a_0 \cos\left(\omega_b t + \phi\right) \tag{2}$$

respectively. In the above A_0 and A_1 are pressure gradient of steady flow and amplitude of oscillatory part, respectively, a_0 is the amplitude of body acceleration, $\omega_P = 2\pi f_P$, $\omega_b = 2\pi f_b$ with f_P is the pulse frequency and f_b is body acceleration frequency, φ is the phase angle of body acceleration G with respect to pressure gradient, and t represents time.

The only governing equation of motion for the flow in cylindrical polar coordinates is given by

$$\rho\frac{\partial u}{\partial t} = -\frac{\partial P}{\partial z} + \rho G + \mu\nabla^2 u - \sigma {B_0}^2 u \tag{3}$$

where u is the axial velocity of blood; P-blood pressure; $\frac{\partial P}{\partial z}$ – pressure gradient; ρ – uniform density of blood; μ – the viscosity of blood; B_0 – the external uniform magnetic field along the radial direction and σ is the conductivity of the blood. Assuming a low magnetic Reynolds number, the induced magnetic field has been neglected.

The geometry of the stenosis, as shown in Figure 1, is given by

$$R(z) = \begin{cases} a - \delta\left(1 + \cos\frac{\pi z}{2z_0}\right), & -2z_0 \le z \le 2z \\ a, & \text{otherwise,} \end{cases}$$

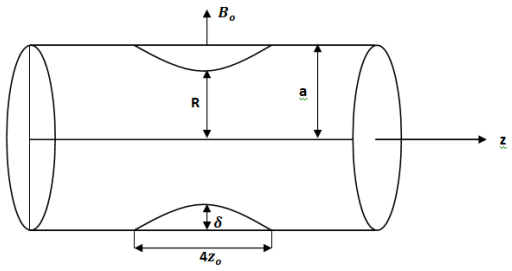

Figure 1: Geometry of artery with stenosis

where R(z) is the radius of the stenosed artery, a is the radius of the artery, is the length of stenosis and 2δ is the maximum protuberance of the stenotic form of the a $4z_0$ rtery wall.

We now introduce a radial coordinate transformation for convenience by the relation

$$\xi = \frac{r}{R(z)},$$

where R(z) depends on δ. The equation (3) then becomes

$$\rho\frac{\partial u}{\partial t} = A_0 + A_1\cos\left(\omega_p t\right) + \rho a_0 \cos\left(\omega_b t + \phi\right) + \frac{\mu}{R^2}\left[\frac{\partial^2 u}{\partial \xi^2} + \frac{1}{\xi}\frac{\partial u}{\partial \xi}\right] - \mu C^2 u \tag{4}$$

where $C = \frac{M}{R}$, $M = \sqrt{\frac{\sigma}{\mu}}RB_0$ (Hartmann number).

Let us consider the case that at t < 0, only the pumping action of the heart is present while the flow in the artery corresponds to the instantaneous pressure gradient at t = 0, i.e.

$$-\frac{\partial P}{\partial z} = A_0 + A_1$$

as a result of which, the flow velocity at t=0 is given by

$$u(\xi,0) = \frac{A_0 + A_1}{\mu C^2}\left[1 - \frac{I_0(CR\xi)}{I_0(CR)}\right] \tag{5}$$

I_0 being the modified Bessel function of the first kind of order zero.

The initial and boundary conditions for the problem are :

$$\left.\begin{aligned} u(\xi,0) &= \frac{A_0 + A_1}{\mu C^2}\left[1 - \frac{I_0(CR\xi)}{I_0(CR)}\right], \\ u &= u_0 \quad \text{at} \quad \xi = 1, \\ &\text{and} \quad u \text{ is finite at } \xi = 0, \end{aligned}\right\} \tag{6}$$

where u_0 is the slip velocity at the stenosed region of the arterial wall.

Solutions

Laplace transforms to equation (4), and the first boundary condition of (6) lead to

$$\rho s\bar{u} - \rho\left[u_0\frac{I_0(CR\xi)}{I_0(CR)} + \frac{(A_0+A_1)}{\mu C^2}\left\{1-\frac{I_0(CR\xi)}{I_0(CR)}\right\}\right]$$

$$= \frac{A_0}{s} + \frac{A_1 s}{\left(s^2+\omega_p^2\right)} + \frac{\rho a_0\left(s\cos\phi - \omega_b \sin\phi\right)}{\left(s^2+\omega_b^2\right)} + \frac{\mu}{R^2}\left[\frac{\partial^2\bar{u}}{\partial\xi^2} + \frac{1}{\xi}\frac{\partial\bar{u}}{\partial\xi}\right] - \mu C^2\bar{u} \tag{7}$$

bar representing the Laplace transform of a function, and s is the transform parameter.

Also, applying the finite Hankel transformation to equation (7), we obtain

$$\bar{u}^*(\lambda_n,s) = \frac{R^2 J_1(\lambda_n)}{\lambda_n\left[\rho sR^2 + \mu\left(C^2R^2+\lambda_n^2\right)\right]}\left[\begin{array}{l}\dfrac{A_0}{s} + \dfrac{A_1 s}{\left(s^2+\omega_P^2\right)} + \\ \dfrac{\rho a_0\left(s\cos\phi - \omega_b\sin\phi\right)}{\left(s^2+\omega_b^2\right)} + \\ \dfrac{\rho\left(A_0+A_1\right)R^2}{\mu\left(C^2R^2+\lambda_n^2\right)}\rho u_0\dfrac{{\lambda_n}^2}{\left(C^2R^2+\lambda_n^2\right)}\end{array}\right] \tag{8}$$

Where $\bar{u}^*(\lambda_n,s) = \int_0^1 r\bar{u}(r,s)J_0(r\lambda_n)dr$ and λ_n are zeros of J_0, the Bessel function of the first kind of order zero and $v = \frac{\mu}{\rho}$.

The Laplace and Hankel inversions of equation (8) in the usual way lead to the final solution for blood velocity as

$$u(\xi,t) = 2\sum_{n=1}^{\infty}\frac{J_0(\lambda_n\xi)R^2}{\lambda_n J_1(\lambda_n)}\left[\left\{\begin{array}{l}\dfrac{A_0}{\mu\left(\lambda_n^2+C^2R^2\right)} + \\ \dfrac{A_1\left[v\left(\lambda_n^2+C^2R^2\right)\cos\omega_p t + \omega_p R^2\sin\omega_p t\right]}{\rho\left[R^4\omega_P^2 + v^2\left(\lambda_n^2+C^2R^2\right)^2\right]}\end{array}\right.\right.$$

$$\left.\left. + \frac{a_0\left[v\left(\lambda_n^2+C^2R^2\right)\cos\left(\omega_b t+\phi\right) + \omega_b R^2\sin\left(\omega_b t+\phi\right)\right]}{R^4\omega_b^2 + v^2\left(\lambda_n^2+C^2R^2\right)^2}\right\}\cdot\right.$$

$$-e^{-\left(\frac{v}{R^2}\right)\left(\lambda_n^2+C^2R^2\right)t}\left\{\frac{-A_1\omega_P^2R^4}{\mu\left(\lambda_n^2+C^2R^2\right)\left[R^4\omega_P^2 + v^2\left(\lambda_n^2+C^2R^2\right)^2\right]}\right.$$

$$\left.\left. + \frac{a_0\left[v\left(\lambda_n^2+C^2R^2\right)\cos\phi + \omega_b R^2\sin\phi\right]}{R^4\omega_b^2 + v^2\left(\lambda_n^2+C^2R^2\right)^2} - \frac{u_0\lambda_n^2}{R^2\left(\lambda_n^2+C^2R^2\right)}\right\}\right] \tag{9}$$

which can also be rewritten in the form

$$u(\xi,t) = \frac{2A_0R^2}{\mu}\sum_{n=1}^{\infty}\frac{J_0(\lambda_n\xi)}{\lambda_n J_1(\lambda_n)}\left[\left\{\begin{array}{l}\dfrac{1}{\left(\lambda_n^2+C^2R^2\right)} \\ + \dfrac{\varepsilon\left(\lambda_n^2+C^2R^2\right)\cos\omega_p t + \alpha^2\sin\omega_p t}{\left(\lambda_n^2+C^2R^2\right)^2+\alpha^4}\end{array}\right\}\right.$$

$$+\frac{\rho a_0}{A_0}\left\{\frac{\left(\lambda_n^2+C^2R^2\right)\cos\left(\omega_b t+\phi\right) + \beta^2\sin\left(\omega_b t+\phi\right)}{\left(\lambda_n^2+C^2R^2\right)^2+\beta^4}\right\}$$

$$-e^{-\left(\frac{v}{R^2}\right)\left(\lambda_n^2+C^2R^2\right)t}\left\{\frac{-\varepsilon\alpha^4}{\left(\lambda_n^2+C^2R^2\right)\left[\alpha^4+\left(\lambda_n^2+C^2R^2\right)^2\right]}\right.$$

$$\left.\left. + \frac{\frac{\rho a_0}{A_0}\left\{\left(\lambda_n^2+C^2R^2\right)\cos\phi + \beta^2\sin\phi\right\}}{\left(\lambda_n^2+C^2R^2\right)^2+\beta^4} - \frac{\frac{\mu u_0}{A_0}\lambda_n^2}{R^2\left(\lambda_n^2+C^2R^2\right)}\right\}\right] \tag{10}$$

Where $\alpha^2 = \frac{\omega_P R^2}{v} = Re_P$, $\beta^2 = \frac{\omega_b R^2}{v} = Re_b$, $\varepsilon = \frac{A_1}{A_0}$

The analytical expression for u consists of four parts. The first and second parts correspond to steady and oscillatory parts of pressure gradient, the third term indicates body acceleration, and the last term is the transient term. As t $\to\infty$, the transient term approaches to zero. Then, from equation (10), we get

$$u(\xi,t) = \frac{2A_0R^2}{\mu}\sum_{n=1}^{\infty}\frac{J_0(\lambda_n\xi)}{\lambda_n J_1(\lambda_n)}\left[\left\{\begin{array}{l}\dfrac{1}{\left(\lambda_n^2+C^2R^2\right)} \\ + \dfrac{\varepsilon\left(\lambda_n^2+C^2R^2\right)\cos\omega_p t + \alpha^2\sin\omega_p t}{\left(\lambda_n^2+C^2R^2\right)^2+\alpha^4}\end{array}\right\}+\right.$$

$$\left.\frac{\rho a_0}{A_0}\left\{\frac{\left(\lambda_n^2+C^2R^2\right)\cos\left(\omega_b t+\phi\right) + \beta^2\sin\left(\omega_b t+\phi\right)}{\left(\lambda_n^2+C^2R^2\right)^2+\beta^4}\right\}\right] \tag{11}$$

The volumetric flow rate Q is given by

$$Q(\xi,t)=2\pi\int_0^R rudr=\frac{4\pi A_0R^4}{\mu}\sum_{n=0}^{\infty}\frac{1}{\lambda_n^2}\left[\left\{\frac{1}{\left(\lambda_n^2+C^2R^2\right)}+\frac{\varepsilon\left(\lambda_n^2+C^2R^2\right)\cos\omega_Pt+\alpha^2\sin\omega_Pt}{\left(\lambda_n^2+C^2R^2\right)^2+\alpha^4}\right\}+\frac{\rho a_0}{A_0}\left\{\frac{\left(\lambda_n^2+C^2R^2\right)\cos\left(\omega_bt+\phi\right)+\beta^2\sin\left(\omega_bt+\phi\right)}{\left(\lambda_n^2+C^2R^2\right)^2+\beta^4}\right\}\right] \quad (12)$$

The fluid acceleration F reads

$$F(\xi,t)=\frac{\partial u}{\partial t}$$

$$=\frac{2A_0}{\rho}\sum_{n=1}^{\infty}\frac{J_0\left(\lambda_n\xi\right)}{\lambda_nJ_1\left(\lambda_n\right)}\left[\left\{\frac{\alpha^2\left\{-\varepsilon\left(\lambda_n^2+C^2R^2\right)\sin\omega_Pt+\alpha^2cos\omega_Pt\right\}}{\left(\lambda_n^2+C^2R^2\right)^2+\alpha^4}\right\}+\frac{\rho a_0\beta^2}{A_0}\left\{\frac{-\left(\lambda_n^2+C^2R^2\right)\sin(\omega_bt+\phi)+\beta^2\cos\left(\omega_bt+\phi\right)}{\left(\lambda_n^2+C^2R^2\right)^2+\beta^4}\right\}\right] \quad (13)$$

The expression for the wall shear stress τ_w can be obtained from

$$\tau_w=\mu\left(\frac{\partial u}{\partial r}\right)_{r=R}$$

as

$$\tau_w(\xi,t)=-2A_0R\sum_{n=1}^{\infty}\left[\left\{\frac{1}{\left(\lambda_n^2+C^2R^2\right)}+\frac{\varepsilon\left(\lambda_n^2+C^2R^2\right)cos\omega_Pt+\alpha^2sin\omega_Pt}{\left(\lambda_n^2+C^2R^2\right)^2+\alpha^4}\right\}+\frac{\rho a_0}{A_0}\left\{\frac{\left(\lambda_n^2+C^2R^2\right)\cos\left(\omega_bt+\phi\right)+\beta^2\sin\left(\omega_bt+\phi\right)}{\left(\lambda_n^2+C^2R^2\right)^2+\beta^4}\right\}\right] \quad (14)$$

Numerical Results

For a given steady-state pressure gradient A_0, fixed values of k and non-zero values of a_0, the variations of the physiologically important fluid dynamic quantities, viz. velocity, volumetric flow rate, wall shear stress, etc., are shown graphically in figures 2(a) to 9(c) for different values of Hartmann number (M), phase angle (φ), time (t), etc. For numerical calculations, we choose, $f_p=1.5, f_b=1.5$, $A_1=0.5A_0$, $\omega_p=2.5\pi$, and the radius of different arteries is shown in Table 1.

The expression for the velocity profile computed in equation (10) has been depicted in figures 2(a) to 5(c) by plotting $\frac{r}{R}$ versus u in the presence/absence of Hartmann number (M) for different values of phase angle (φ) and time t. It is observed that velocity decreases with increasing Hartmann number (M) is blunted near the axis of the artery, and decreases rapidly with respect to $\frac{r}{R}$ i.e., with respect to r.

Table 1: Radius of different arteries

Blood vessels	*Radius(cm)*
Aorta	1.2
Femorat	0.6
Carotid	0.3
Coronary	0.15
Arteriole	0.008

Again, the maximum axial velocity depends on tube diameter, i.e., the velocity increases as tube diameter increases from the arteriole to the aorta. Also, it is seen that blood velocity decreases with the increase in phase angle (φ) for different arteries.

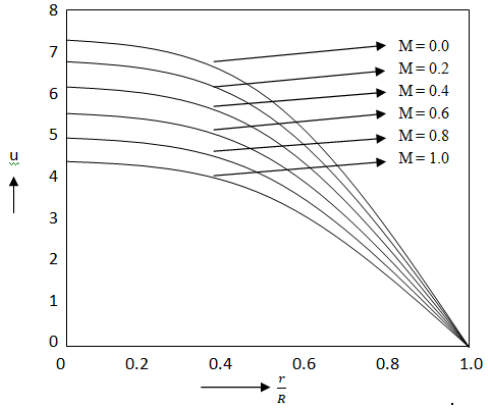

Figure 2-a: Variation of velocity profiles for aorta artery against $\frac{r}{R}$ with $\varphi=0$, t = 0.

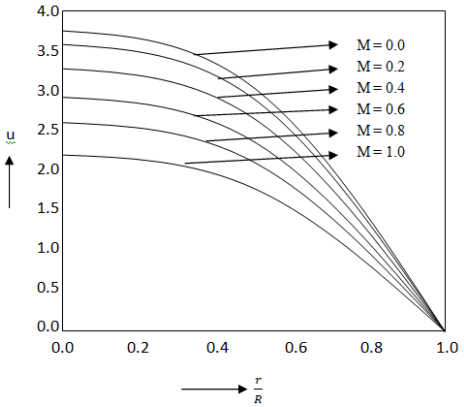

Figure 2-b: Variation of velocity profiles for femorat artery against $\frac{r}{R}$ with $\varphi=0$, t = 0.

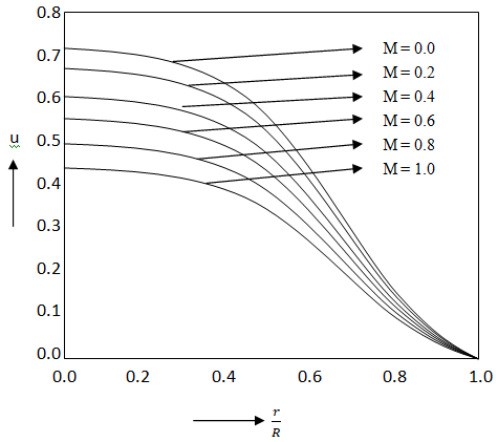

Figure 2-c: Variation of velocity profiles for coronary artery against $\frac{r}{R}$ with $\varphi = 0$, t = 0 .

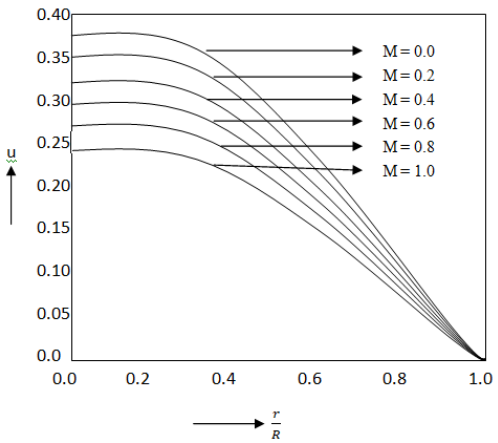

Figure 3-c: Variation of velocity profiles for coronary artery against $\frac{r}{R}$ with $\varphi = 0$, t = 30 .

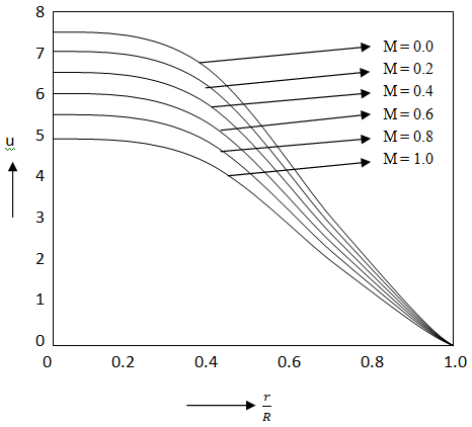

Figure 3-a: Variation of velocity profiles for aorta against $\frac{r}{R}$ with $\varphi = 0$, t = 30.

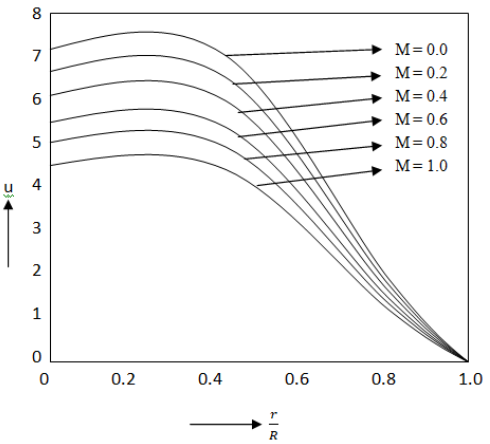

Figure 4-a: Variation of velocity profiles for aorta artery against $\frac{r}{R}$ with $\varphi = 30$, t = 0 .

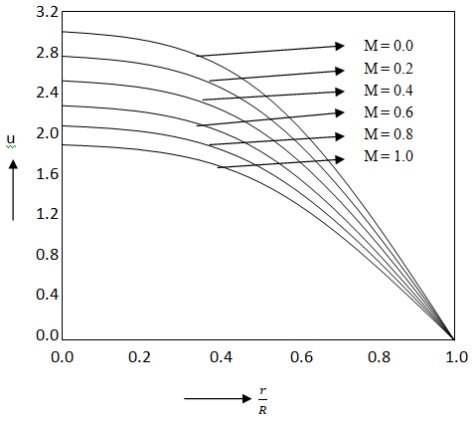

Figure 3-b: Variation of velocity profiles for femoral artery against $\frac{r}{R}$ with $\varphi = 0$, t = 30.

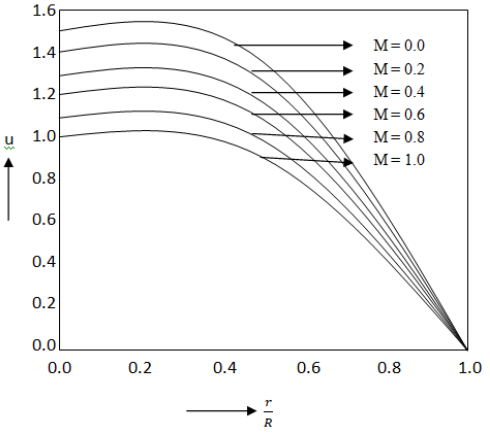

Figure 4-b: Variation of velocity profiles for femorat artery against $\frac{r}{R}$ with $\varphi = 30$, t = 0 .

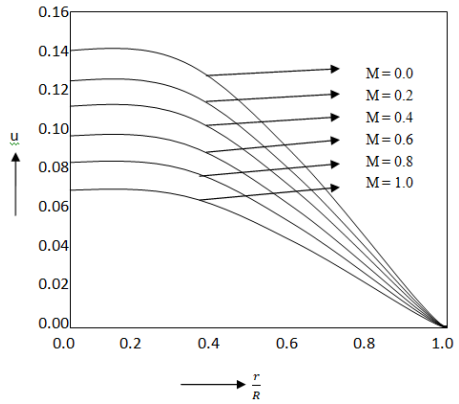

Figure 4-c: Variation of velocity profiles for coronary artery against $\frac{r}{R}$ with $\varphi = 30$, t = 0 .

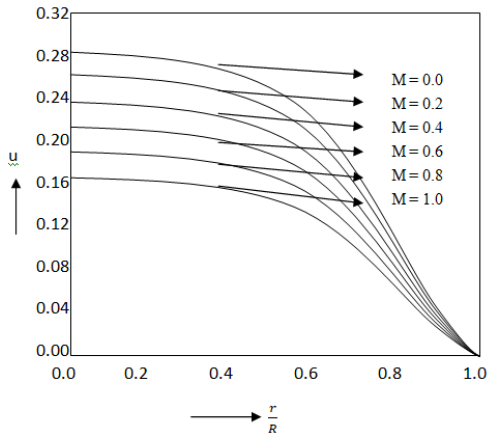

Figure 5-c: Variation of velocity profiles for coronary artery against $\frac{r}{R}$ with $\varphi = 60$, t = 30 .

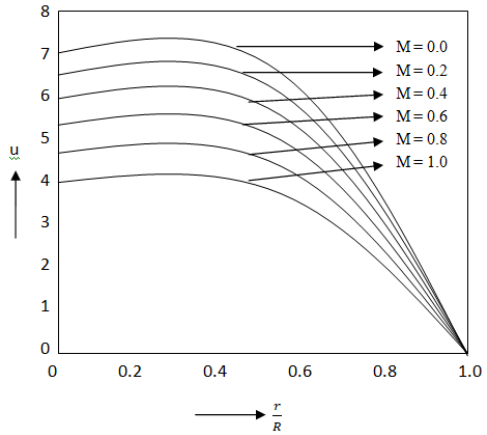

Figure 5-a: Variation of velocity profiles for aorta artery against $\frac{r}{R}$ with $\varphi = 60$, t = 30 .

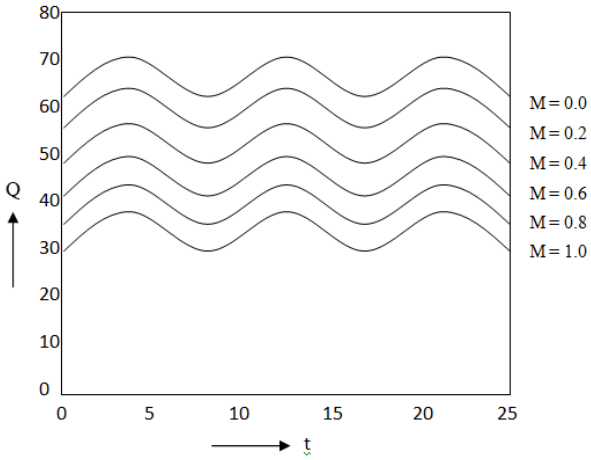

Figure 6-a: Variation of flow rate for aorta artery against t when φ = 30.

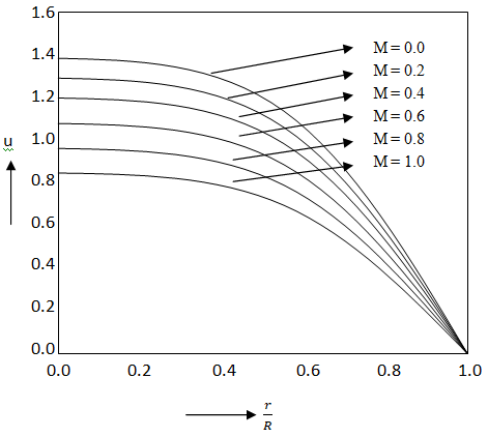

Figure 5-b: Variation of velocity profiles for femorat artery against $\frac{r}{R}$ with $\varphi = 60$, t = 30 .

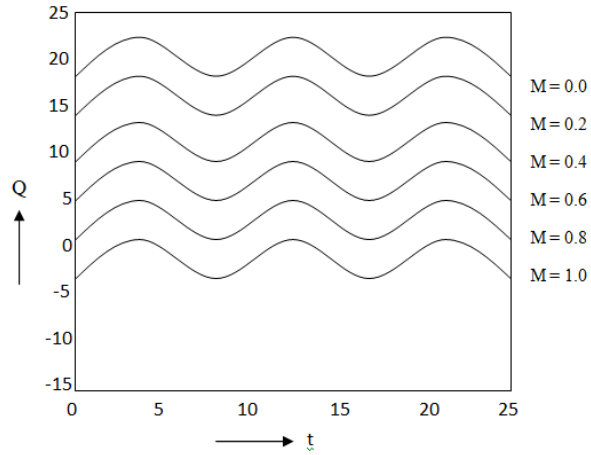

Figure 6-b: Variation of flow rate for femorat artery against t when φ=30

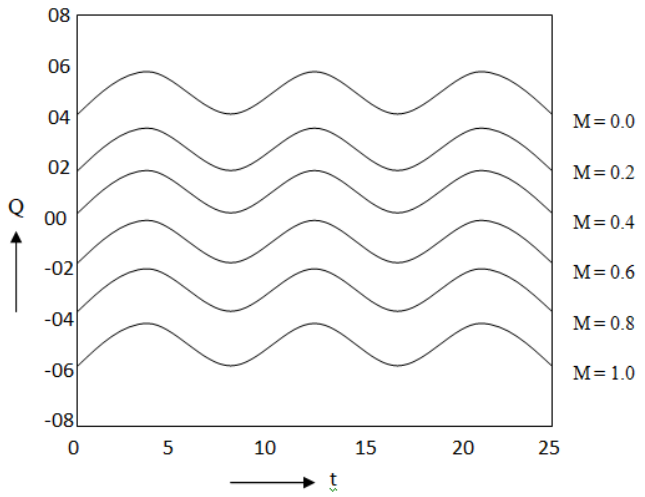

Figure 6-c: Variation of flow rate for coronary artery against t when φ = 30.

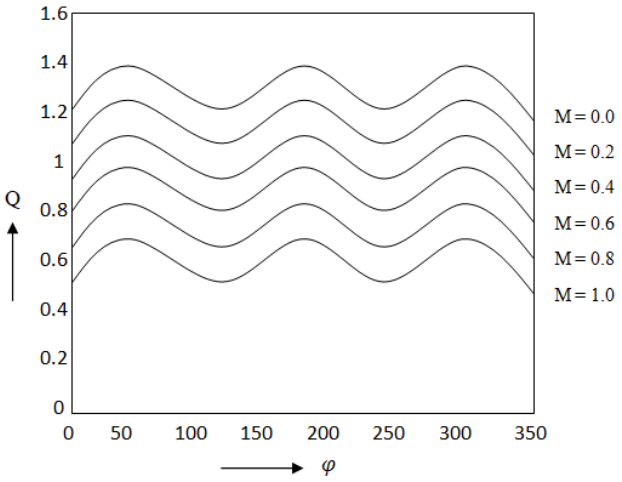

Figure 7-b: Variation of flow rate for femorat artery against φ when t = 30

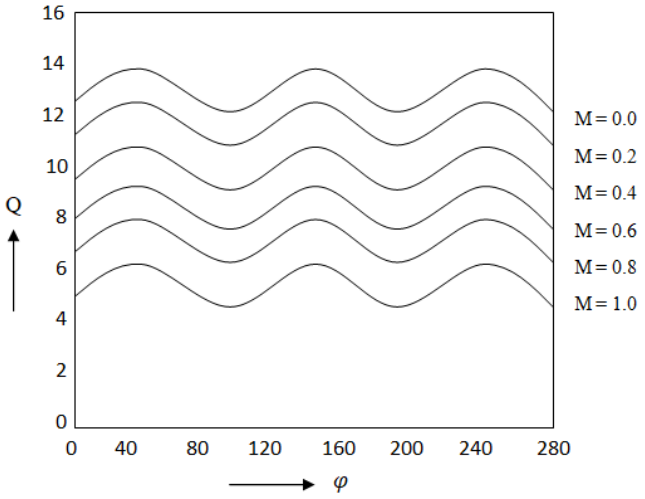

Figure 7-a: Variation of flow rate for aorta artery against φ when t = 30.

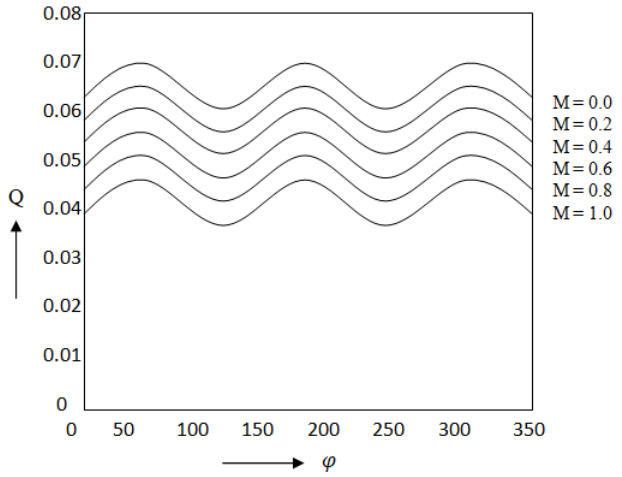

Figure 7- c: Variation of flow rate for coronary artery against φ when t = 30

The volumetric flow rate Q has been shown in figures 6(a) to 6(c) for different values of Hartmann number (M). For fixed value of φ, it is observed that increase in M decreases the maximum value of the flow rate Q and the oscillatory nature of the curves with time is nearly same for different values of M. Figures 7(a) to 7(c) show that flow rate Q decreases with increase of Hartmann number (M) at the given time for various phase angle φ and it decreases more rapidly with the decrease of the radius of the artery.

Figures 8(a) to 9(c) indicate the effect of Hartmann number on wall shear stress τ_w. For fixed value of φ, it is found from figures 8(a) to 8(c) that the maximum value of the wall shear stress decreases with increase in M whereas from 9(a) to 9(c), it is clear that for fixed value of t, the maximum value of τ_w increases with increase in M. In both cases, wall shear stress decreases with increasing the radius of the artery.

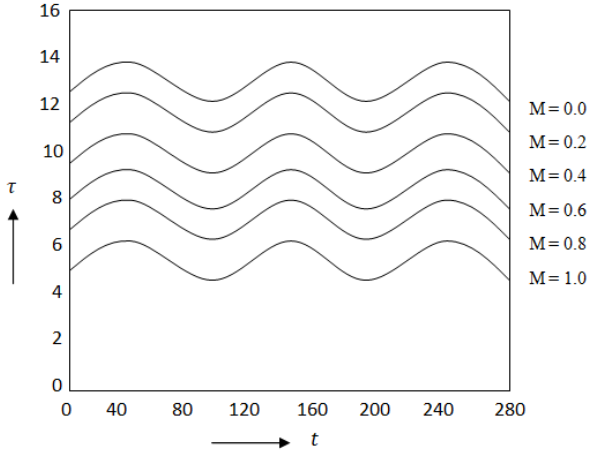

Figure 8-a: Variation of wall shear stress for aorta artery against t when φ= 30

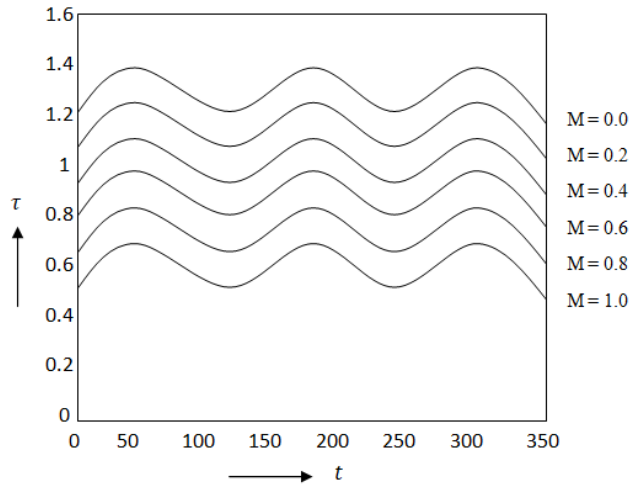

Figure 8-b: Variation of wall shear stress for femorat artery against t when φ = 30

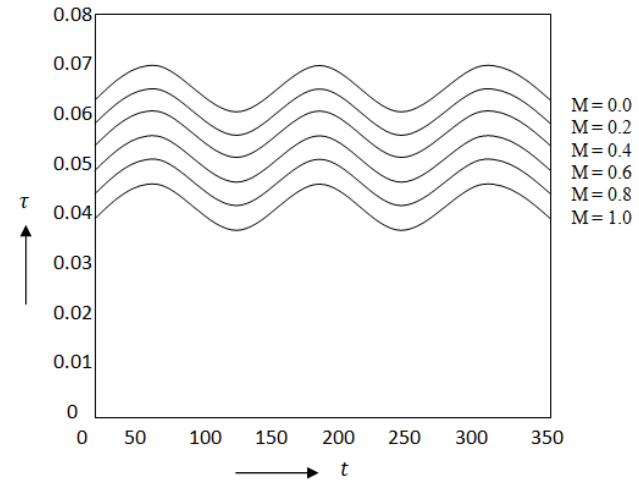

Figure 8-c: Variation of wall shear stress for coronary artery against t when φ = 30

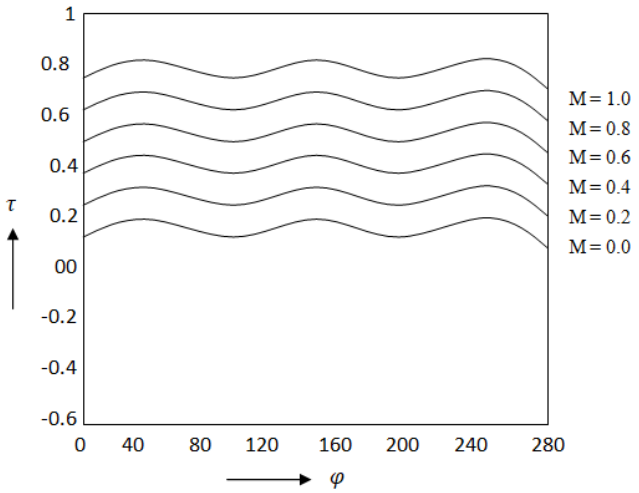

Figure 9-a: Variation of wall shear stress for aorta artery against t when t = 30

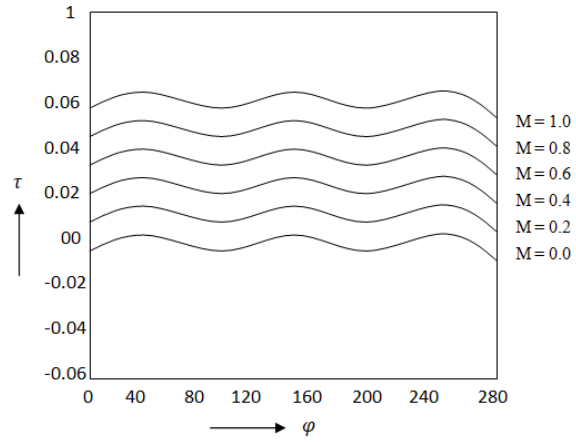

Figure 9-b: Variation of wall shear stress for femorat artery against t when t = 30

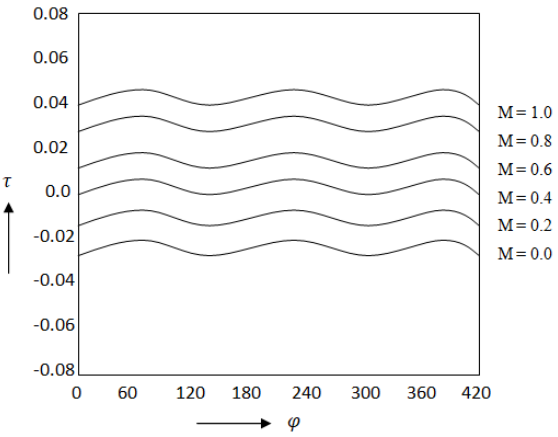

Figure 9-c: Variation of wall shear stress for coronary artery against t when t = 30

CONCLUSION

Using the available physiological data, it is observed from the above analysis that the blood velocity and maximum value of volumetric flow rate decreases with increasing Hartmann number and given phase angle; however, the flow rate curves are oscillating in nature. A very interesting feature has been observed in the study and the slip velocity has no effect for large values of time.

REFERENCES

1. Sud VK, Sekhon GS. Arterial flow under periodic body acceleration. *Bull Math Biol.* 1985;47(1):35-52. DOI: 10.1007/BF02459645
2. Young DF. Fluid mechanics of arterial stenosis. *J Bio Mech Engng (Trans AMES).* 1979; 101:157-75. DOI: 10.1115/1.3426241
3. Coklet GR. The rheology of human blood. Fung YC(Eds.), *Biomechanics,* Prentice-Hall, Englewood Cliffs, 1972. Available at: http://www.gaitlab.ir/books/gaitlab_ref_22_Biomechanics:_

Mechanical_Properties_of_Living_Tissues.pdf
4. Vardanyan VA. Effect of magnetic field on blood flow. *Bio. Physics*. 1973;18:515-21. PMID: 4717778.
5. Chaturani P, Biswas DA. A comparative study of two-layered Poiseuille flow of a polar fluid under different boundary conditions with application to blood flow. In: Proceedings of the Ninth International Congress of Mathematical Biology, 1983, at Paris, France. Biorheol. Revue de Bio-Mathematique. 1988;101:47-56.
6. Omamoke E, Amos E. Slip and pulsatile MHD blood flow through an inclined stenosed artery with body acceleration and heat source effects. *IOSR J Math*. 2022;18(1, SERIES 2):1-23. DOI:10.9790/5728-1801020123.
7. Nandal J, Kumari S, Rathee R. The effect of slip velocity on unsteady peristalsis MHD blood flow through a constricted artery experiencing body acceleration. *Int J Appl Mechanics Eng*. 2019;24(3):645-59. DOI: 10.2478/ijame-2019-0040.
8. Islam M. Eldesoky V. Slip effects on the unsteady MHD pulsatile blood flow through porous medium in an artery under the effect of body acceleration. *Int J Math Mathematical Sci*. 2012;2012:860239. DOI:1155/2012/860239.
9. Changdar S, De S. Analytical investigation of nanoparticle as a drug carrier suspended in a MHD blood flowing through an irregular shape stenosed artery. *Iran J Sci Tech Trans Sci*. *2019;43:1259-72*. DOI: 10.1007/s40995-018-0601-1
10. Changdar S, Mandal AK, De S. Analytical investigation of non-spherical nanoparticle as a drug agent suspended in a magnetohydrodynamic blood nanofluid flowing through an irregular-shape stenosed artery. *J Nanofluids*. 2018;7(6):1187-94. DOI: 10.1166/jon.2018.1526
11. Medvedev A E. Two phase blood-flow model. *Russ J Biomech*. 2013;17:18-32. Available at: https://www.researchgate.net/publication/271512129_Two-phase_blood-flow_model
12. Sanyal DC, Das, K. Debnath S. Effect of magnetic field on pulsatile blood flow through an inclined circular tube with periodic body acceleration. *J Phys Sci*. 2007;11:43-56. Available at: https://ir.vidyasagar.ac.in/bitstream/123456789/744/2/JPS11-05.pdf.
13. Rathod VP, Shakara T, Itagi SR, Rajput GG. Pulsatile flow of blood under the periodic body acceleration with magnetic field. *Ultra Scientist of Physical Sciences*. 2005;17(1):7-16. Available at: https://www.researchgate.net/publication/233926735.
14. Shahawey EI, Elsayed EF, Ealbarbary ME, Afifi NAS, Mostafa E. MHD flow of an elastic-viscous fluid under periodic body acceleration. *Int J Math Sci*. 2000;23(11):795-9. Available at: https://www.emis.de/journals/HOA/IJMMS/Volume23_11/717908.pdf.
15. Bhuvan BC, Hazarika GC. Effect of magnetic field on Pulsatile flow of blood in a porous channel. *Bio-Sci Res Bull*. 2001;17(2):105-11.
16. Bennet L. Red cell slip at a wall in vitro, *Science*. 1967;155: 1554-6. DOI: 10.1126/science.155.3769.1554.
17. Chaturani P, Palanasamy V. Pulsatile flow of blood with periodic body acceleration. *Int J Engng Sci*. 1991;29(1):113-21. DOI: 10.1016/0020-7225(91)90081-D.
18. Berger SA, Jou LD. Flow sinstenotic vessels. *An nualre view of fluid mechanics*. 2000;32: 347-82. Available at: https://www.annualreviews.org/content/journals/10.1146/annurev.fluid.32.1.347.
19. Shahawey EI, Elsayed EF, Afifi NAS. Pulsatile flow of blood through a porous medium under periodic body acceleration. *Int J Theor Phys*. 2000;39(1):183-8. DOI:10.1023/A:1003611604207
20. Vardanian VA. Vliianie magnitnogo polia na techenie krovi [Effect of a magnetic field on blood flow]. Biofizika. 1973;18(3):491-6. Russian. PMID: 4717778.
21. Das K, Saha GC. Arterial MHD Pulsatile flow of blood under the periodic body acceleration. *Bull Soc Math Banja Luka*, 2009;16:21-42.Available at: http://www.imvibl.org/imvibl/buletin/buletin_16_2009/bul_soc_mat_bl_16_2009_21-42.pdf.

PEER-REVIEWED CERTIFICATION

During the review of this manuscript, a double-blind peer-review policy has been followed. The author(s) of this manuscript received review comments from a minimum of two peer-reviewers. Author(s) submitted revised manuscript as per the comments of the assigned reviewers. On the basis of revision(s) done by the author(s) and compliance to the Reviewers' comments on the manuscript, Editor(s) has approved the revised manuscript for final publication.